Available online at www.sciencedirect.com
SCIENCE DIRECT®
Journal of Power Sources 118 (2003) 71–78
JOURNAL OF POWER SOURCES
www.elsevier.com/locate/jpowsour

Development of a methanol fuelled reformer for fuel cell applications

Bård Lindström, Lars J. Pettersson*

Department of Chemical Engineering and Technology, Chemical Technology, KTH-Royal Institute of Technology, SE-100 44 Stockholm, Sweden

Abstract

A compact methanol reformer for fuel cell vehicles (FCVs) has been developed and successfully tested. The reformer which has been constructed to serve a 5 kWe fuel cell operates by combined reforming of methanol (CRM) (a combination of steam reforming and partial oxidation). The exploitable energy surplus in a fuel cell vehicle is low and therefore a combustion system for heating the reformer which utilizes a catalyst for both evaporation and oxidation of liquid methanol was developed. We were able to obtain start-up times in the region of 4–6 min depending on the oxygen-to-methanol ratio (OMR) used for the combined reforming reaction. The main drawback from decreasing the start-up time by increasing the oxygen-to-methanol ratio was that the CO concentrations in the product stream increased. The reforming reaction was performed over copper-based catalysts while the oxidation took place over a mixture of platinum and manganese-based catalysts. The catalysts were characterized using SEM-EDS, BET surface area measurement and X-ray diffraction (XRD).

Keywords: Methanol; Reformer; Fuel cell; Start-up; Steam reforming; Catalyst

1. Introduction

The search for alternative propulsion systems for automobiles has been extensive during the last decade as a result of concerns over health issues, global warming and desires to conserve oil reserves. Vehicles powered by fuel cells are currently considered by the automotive industry as a realistic alternative to the internal combustion engine (ICE).

The ideal fuel cell vehicle (FCV) would run on pure hydrogen (H_2) stored on-board the vehicle, however technological limitations in the storage capacity of pure hydrogen do not permit enough H_2 to be stored to provide the performance expected by consumers. The required H_2 can instead be generated on-board the vehicle from alternate hydrogen carriers such as methanol and gasoline.

Anthropogenic emissions of carbon dioxide (CO_2) from the transportation sector can be reduced by up to 50% by replacing the ICE with a methanol-based fuel cell power system [1]. In addition, there are practically no NO_x, SO_x or hydrocarbons emitted from a fuel cell powered system which utilizes processed methanol for fuelling the fuel cell. The implementation of methanol fuel cell vehicles (MFCV) is therefore an effective method for reducing emissions.

For fuel cell applications there are three processes available for extracting H_2 from methanol: (i) steam reforming of methanol (SRM), (ii) partial oxidation of methanol (POM) and (iii) combined reforming of methanol (CRM).

The SRM reaction (Eq. (1)) is a highly developed and thoroughly studied process [2–9] and it is possible to yield a product gas containing up to 75% hydrogen while maintaining a high selectivity towards carbon dioxide. The main drawback of the steam reforming process is that it is slow and endothermic and as result significant amounts of heat has to be provided to maintain the reforming reaction.

POM is a highly exothermic process (Eq. (2)), which can be used to construct highly dynamic and fast reforming systems [10–16]. The formation of hot-spots is one of the main drawbacks from using the partial oxidation process as the formation of these hot-zones in the catalyst can result in sintering and thus lowering the catalyst activity.

The partial oxidation process can theoretically at full conversion generate a product stream containing up to 67% hydrogen. However, for automobile solutions the oxygen will most likely be supplied using compressed air which results in a dilution of the product stream with nitrogen and subsequently lowering the maximum hydrogen concentration to 41%. This is a clear disadvantage since the performance of the fuel cell is dependent on the hydrogen concentration [17].

* Corresponding author. Tel.: +46-8-790-8259; fax: +46-8-10-8579.
E-mail address: larsp@ket.kth.se (L.J. Pettersson).

0378-7753/03/$ – see front matter
doi:10.1016/S0378-7753(03)00064-8

The combined process is a combination of SRM and POM where the oxygen (O_2), water (H_2O) and methanol are co-fed at various ratios. The ratio of the reactants is usually chosen so that the reaction is slightly exothermic or thermally neutral (auto-thermal reforming). By combining POM and SRM it is possible to obtain a system which is dynamic while generating relatively high hydrogen concentrations [1,18–21] as well as avoiding the formation of hot-spots in the catalyst bed. Under optimal conditions SRM and POM produce almost stoichiometric amounts of H_2 and CO_2.

The reactions are described by the following equations:

$$\text{SRM}: \quad CH_3OH + H_2O \rightarrow 3H_2 + CO_2 \tag{1}$$

$$\text{POM}: \quad CH_3OH + \tfrac{1}{2}O_2 \rightarrow 2H_2 + CO_2 \tag{2}$$

$$\text{CRM}: \quad CH_3OH + (1-x)H_2O + \tfrac{1}{2}xO_2 \rightarrow (3-x)H_2 + CO_2 \tag{3}$$

The polymer electrolyte fuel cell (PEFC) which is currently considered as the most feasible fuel cell for automotive applications is highly sensitive to carbon monoxide (CO), which poisons the platinum (Pt) catalyst on the anode. CO has detrimental effects on the performance of the fuel cell at concentrations above 50 ppm.

The CO concentration can be reduced by adding a clean-up step after the fuel processor. The water gas shift (WGS) reaction (Eq. (4)) and the preferential oxidation (PROX) reaction (Eq. (5)) are considered as the most viable clean-up processes available today for automotive fuel cell applications. The low CO tolerance of the fuel cell implies that the size and cost of the fuel processor is dependent on the CO concentration in the product stream.

$$CO + H_2O \rightarrow H_2 + CO_2 \tag{4}$$

$$CO + \tfrac{1}{2}O_2 \rightarrow CO_2 \tag{5}$$

The exploitable energy surplus in a fuel cell vehicle is low and therefore one of the most important tasks is to provide the heat required for the evaporation and conversion of methanol and water. In a previous study, we showed that it was possible to use methanol combustion (Eq. (6)) as an indirect heat source [22].

$$CH_3OH(l) + \tfrac{3}{2}O_2 \rightarrow CO_2 + 2H_2O \tag{6}$$

The combustion of methanol is a highly developed process [23–25], however as we are using liquid methanol in the feed to lower the energy requirements of the reformer the experiences from conventional combustion of evaporated methanol are not always applicable for this specific problem.

In order to simplify the design of the fuel processor, a Pt-based catalyst which allows the combustion reactor to be used for combusting both H_2 and methanol has been developed (see Fig. 1) [22]. The activity of the catalyst is such that ignition is obtained when liquid methanol is sprayed together with air onto the catalyst surface. When the reforming system reaches steady state unreacted H_2 from the anode off-gas in the fuel cell can replace the methanol in the combustor. The combustor provides faster start-up times as well as increasing the operating efficiency of the FCV at steady state.

The objective of this study was to develop and construct a self-sustainable compact methanol fuel processor for serving a 5 kWe (kW electric) PEFC. Efforts were made to optimise the fuel processor with respect to start-up time and CO_2 selectivity.

2. Experimental methods

2.1. Catalyst preparation

The catalysts used in these experiments were all based upon spherical γ-alumina pellets from SASOL, Germany (2.5 mm). The catalysts were prepared using wet impregnation [26].

2.1.1. Reforming and shift catalysts

The metallic precursors were all in the form of nitrates and the pH of the nitrate solution was kept above the iso-electric

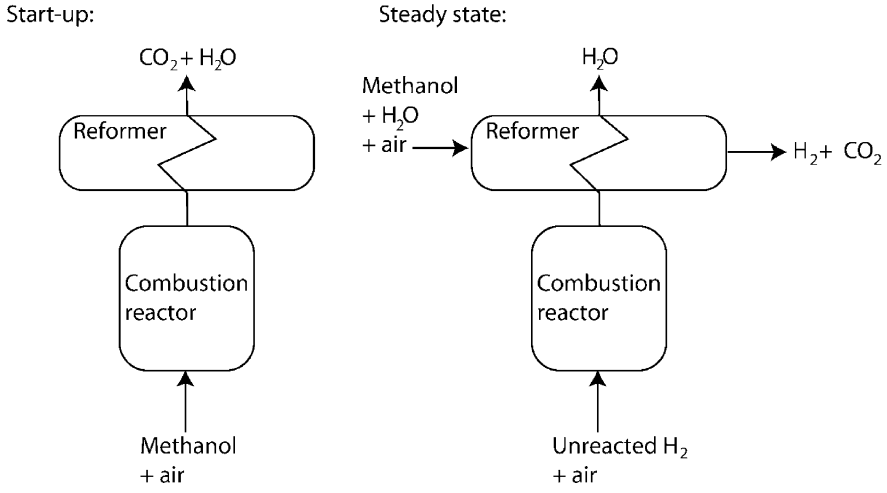

Fig. 1. Principle of operation for start-up and steady state for reformer system.

Table 1
Catalyst sample composition (wt.%)

Reforming catalyst	Combustion catalyst	Shift catalyst
Cu_{40}/Zn_{60}	Pt_{100}	Cu_{40}/Zn_{60}
$Cu_{39}/Zn_{59}/Zr_2$	$Pt_{10}Mn_{90}$	

point of γ-alumina. The pellets were subsequently dried for 12 h at 120 °C prior to calcination. The pellets were then calcined for 5 h at 350 °C. Prior to activity evaluation, the catalysts were reduced in a 10% H_2 in N_2 mixture at a heating rate of 5 °C min^{-1} and dwelling at 220 °C for 2 h. X-ray diffraction confirmed that all copper oxide had been reduced to copper crystals while promoters remained as metallic oxides. Two types of reforming catalysts (see Table 1) were prepared for operation in different regions in the catalyst bed. The catalysts were both promoted by zinc oxide (ZnO) and the second reforming catalyst was also doped with zirconium dioxide (ZrO_2). The composition of the WGS catalysts was identical to the primary reforming catalyst.

2.1.2. Combustion catalyst

The manganese (Mn) precursor was in the form of nitrate and the platinum precursor was platinum(II) 2,4-pentanedionate. The pH of the solutions was kept above the isoelectric point of γ-alumina. The pellets were subsequently dried for 12 h at 120 °C prior to calcination. The pellets were then calcined for 5 h at 600 °C. X-ray diffraction was applied to the catalysts after calcination to identify the crystal phase present in the bulk. For the combustion reaction, a primary ignition catalyst containing Pt was applied to 1/3 of the bed and a secondary combustion catalyst containing Pt–Mn to the rest of the bed (see Table 1).

When referring to the catalysts in this paper, the following notation is used: $A_xB_yC_z$ where x, y and z is the wt.% of components A, B and C (when present). All catalysts were supported on γ-Al_2O_3. The catalysts prepared and tested are listed in Table 1.

2.2. X-ray diffraction

X-ray powder diffraction (XRD) was applied to identify the crystal phases using a Siemens Diffraktometer 5000. The operating parameters were: monochromatic Cu Kα radiation, Ni filter, 30 mA, 40 kV, 2θ scanning from 10 to 90°, and a scan step size of 0.02. Phase identification was done using the reference database (JCPDS-files) supplied with the equipment.

2.3. BET surface area measurements

The specific surface areas of the various samples were measured according to the Brunauer–Emmett–Teller method (BET) by nitrogen adsorption using a Micrometrics ASAP 2010 instrument. Prior to adsorption measurements, the samples were degassed for at least 12 h at 250 °C.

2.4. Fuel processor specification and activity measurements

For this study, a prototype was developed to serve a 5 kWe fuel cell. When determining the required hydrogen flow

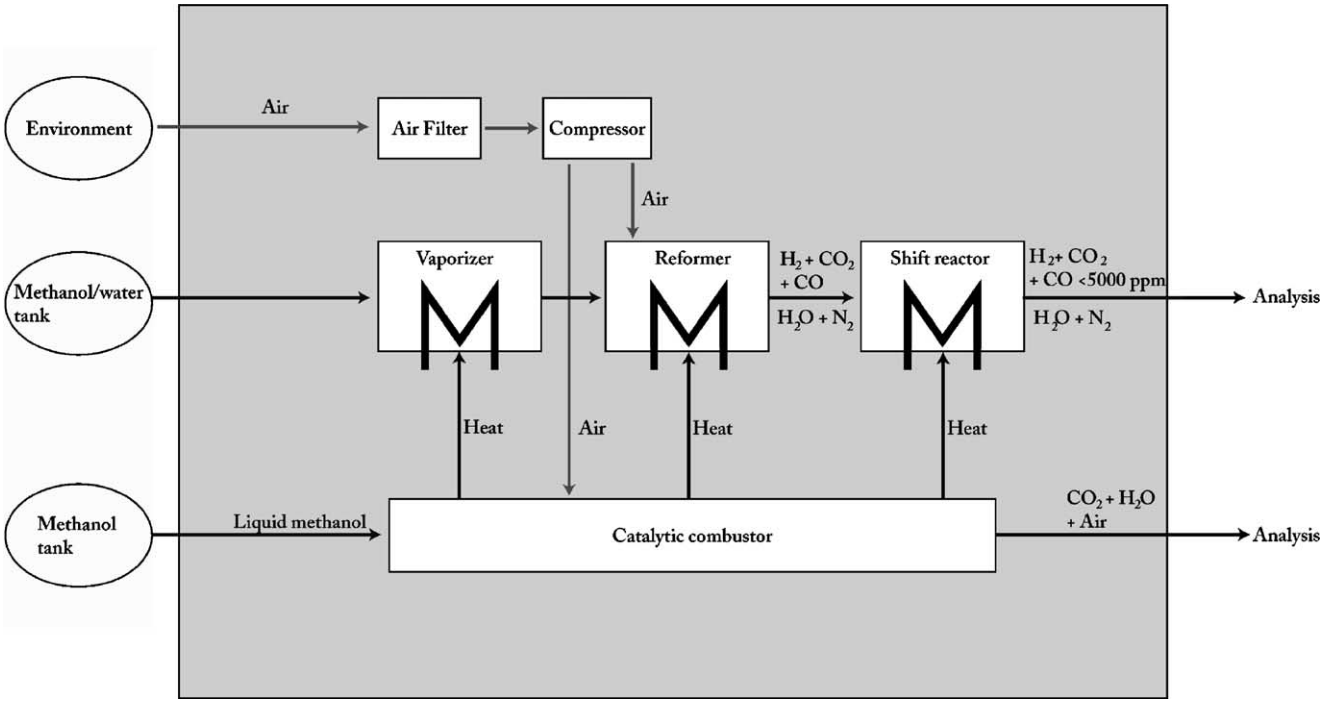

Fig. 2. Outline of fuel processing system.

rates, calculations were made with the heating value of hydrogen while assuming that the efficiency of the fuel cell is 50%. The required hydrogen flow per kWe was then found to be approximately 1000 Ndm^3/h.

The fuel processor (see Fig. 2) consists of four separate modules: (i) catalytic combustor, (ii) vaporizer, (iii) reformer and (iv) shift reactor.

Initially, liquid methanol and air is fed to the catalytic combustor, which utilizes the catalyst for both evaporation and oxidation (see Fig. 3). This is in contrast to traditional reactor systems where the reactants are preheated and the reactor temperature is controlled by a furnace. The catalysts designed for this system must for this reason be bifunctional which increase the requirements on the catalyst, with respect to activity and selectivity, compared to conventional oxidation catalysts.

This unique solution has been adopted since there is no electrical energy available for vaporization and heating in a fuel cell vehicle. The basic principles of the catalytic combustor are as follows.

Liquid methanol is mixed with air in a nebulizer to form a mist of finely divided droplets. The mixture is then passed over the catalyst bed where evaporation and oxidation takes place. The nebulizer is situated in a separate chamber below the catalyst bed in order to allow unreacted methanol to flow back to the nebulization chamber to prevent drenching of the catalyst. The combustor was operated at a gas hourly space velocity (GHSV) of 25,000 and excess air ($\lambda = 6$), to avoid superheating of the system.

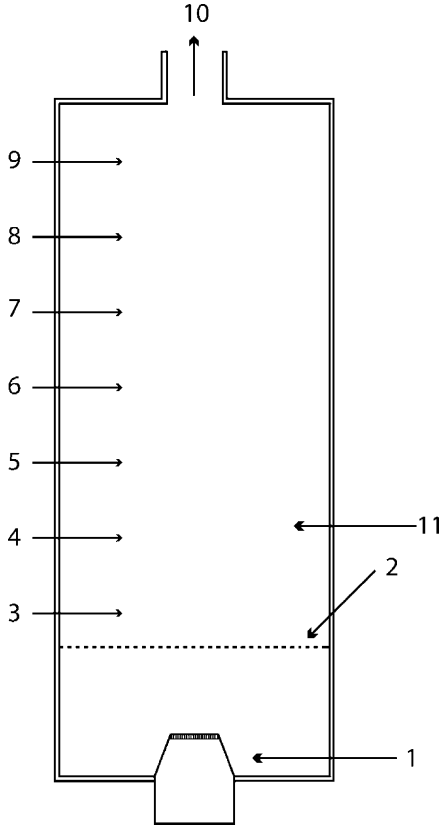

Fig. 3. Laboratory reactor (1, nebulizer; 2, grid separating catalyst chamber from nebulizer; 3–9, thermocouples; 10, effluent; and 11, catalyst bed).

The combusted methanol is subsequently applied as a heating medium to raise the temperature in the other modules. Once the desired operating temperature has been reached in the modules, methanol and water is co-fed to the vaporizer. The methanol–steam combination is thereafter combined with the air in a separate chamber prior to entering the reformer. The reformed gas is then passed through a WGS reactor for CO removal before analysis. The reformer was operated with CMR with an oxygen-to-methanol ratio (OMR) of 0.15 ($\Delta H^\circ = -23.0$ kJ/mol). The OMR of 0.15 was chosen in order to have a process, which was slightly exothermic while maintaining a relatively high theoretical maximum hydrogen (H_2) concentration. The steam-to-methanol ratio was 1.3 which has been shown in earlier work to be optimal for the CMR with respect to activity and selectivity [27]. The GHSV in the reformer was 8000 unless stated otherwise.

All components of the fuel processor were constructed in stainless steel (ASTM 316) and the product stream composition was measured on-line using a gas chromatograph from Varian equipped with both a thermal conductivity detector (TCD) and a flame ionization detector (FID).

3. Results and discussion

3.1. X-ray diffraction

The results of the XRD analysis of the catalysts indicated that the reduction process (Eq. (7)) applied on the copper-based catalysts was sufficient as copper (Cu) was only detected in metallic form (Cu^0). We also performed XRD on the copper-based catalysts from different segments of the bed after activity evaluation and found that the catalysts located closest to the injection point (30% of catalyst bed) had been reoxidized to copper oxide (CuO).

$$CuO + H_2 \rightarrow Cu^0 + H_2O \quad (7)$$

The test showed that Pt existed in metallic form and Mn as MnO_2.

3.2. BET surface area measurements

The BET measurements showed that all catalysts had a surface area between 103 and 108 m^2/g and was primarily used to verify that the scaled-up catalyst manufacturing process yielded the same physical characteristics as in previous studies.

3.3. Evaluation of the catalytic reformer

3.3.1. Catalytic activity and selectivity

The overall performance of a methanol fuelled fuel cell system is unavoidably dependent on the performance of the

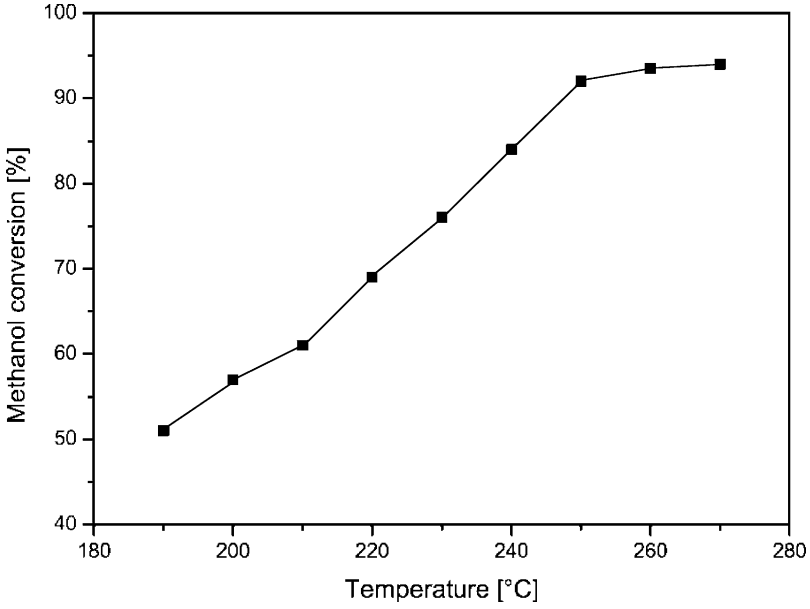

Fig. 4. Methanol conversion as a function of temperature.

reforming catalyst. In a previous study [27], the influence of the copper loading and promoter was investigated for CMR, and it was found that the catalyst with 40 wt.% Cu was most active. In another study [28], we confirmed the results of Breen et al. [4] that zirconium had positive effects on the CO_2 selectivity. The composition of the catalytic bed in the reformer is for this reason a mixture of the $Cu_{40}Zn_{60}$ and the $Cu_{39}Zn_{59}Zr_2$ catalysts.

The reforming reaction is strongly dependent on the temperature as seen in Fig. 4, where the methanol conversion is plotted against the average bed temperature. The conversion exceeds 90% only at temperatures above 250 °C. The rate of H_2 generated (Fig. 5) follows the same trend.

The CO concentration in the reformed gas (see Fig. 6) unfortunately increases with temperature and reaches 5000 ppm at 260 °C. The reformer was chosen to operate at 260 °C, in order to obtain high activity while generating acceptable levels of CO.

3.3.2. *Reformer start-up and stability*

The start-up of the reformer system can be seen as a sequence of steps. Initially the cold methanol and air is introduced to the combustion catalysts, where the methanol evaporates on the catalyst surface and then reacts with the oxygen while generating heat. The temperature then quickly rises in the combustor and reformer (see Fig. 7) and stable

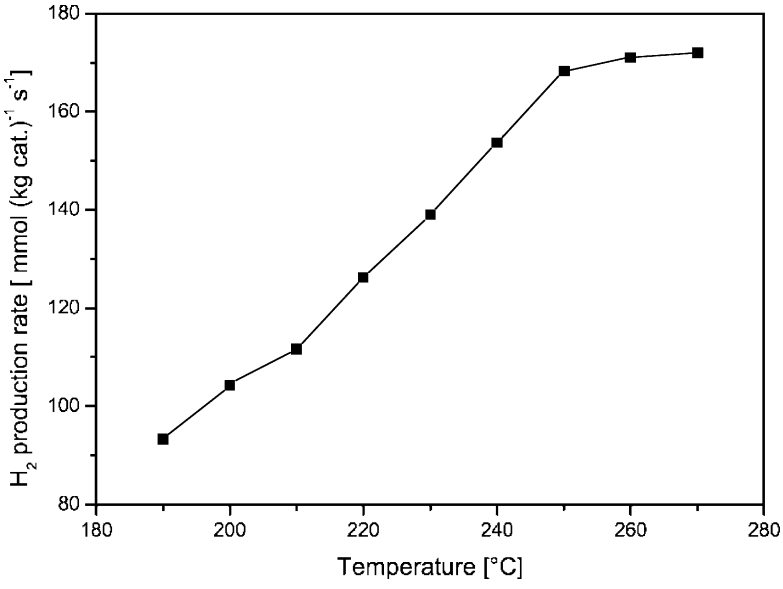

Fig. 5. Hydrogen production rate as a function of temperature.

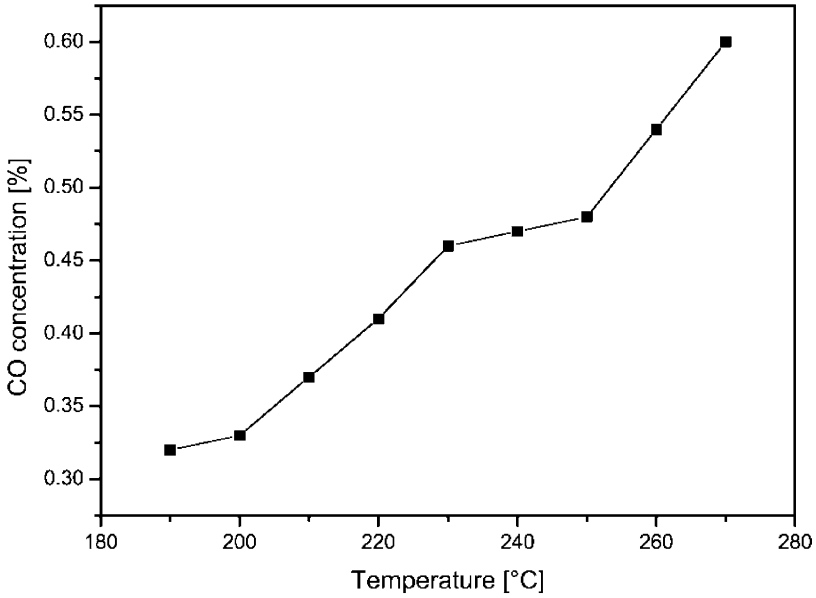

Fig. 6. CO concentration as a function of temperature.

temperature is obtained in the combustor after 300 s. The methanol, water and air mixture is injected into the reformer at $t = 350$ s and as a result of the slightly exothermic nature of the CMR the average reactor temperature increases slightly and the reformer operates at full power after 400 s.

The start-up time can be decreased by increasing the oxygen-to-methanol ratio in the reformer (see Fig. 8). The shorter start-up time is however obtained at the cost of increasing CO concentrations in the product stream. The increase in the CO concentration is most likely attributed to the overall increase in reaction temperature as the thermodynamics of the WGS reaction is favorable at low temperatures [29]. Increasing the CO in the reformed gas implies that the size and cost of the cleanup reactors will increase and thereby the total cost of the fuel cell system will increase. In the end one will have to weigh the start-up time against the cost and decide which factor will be most crucial for the consumer.

The stability of the system was studied for a period of 12 h, where we see in Fig. 9 that the conversion and product concentrations were stable (within the error margin of the analyzing equipment).

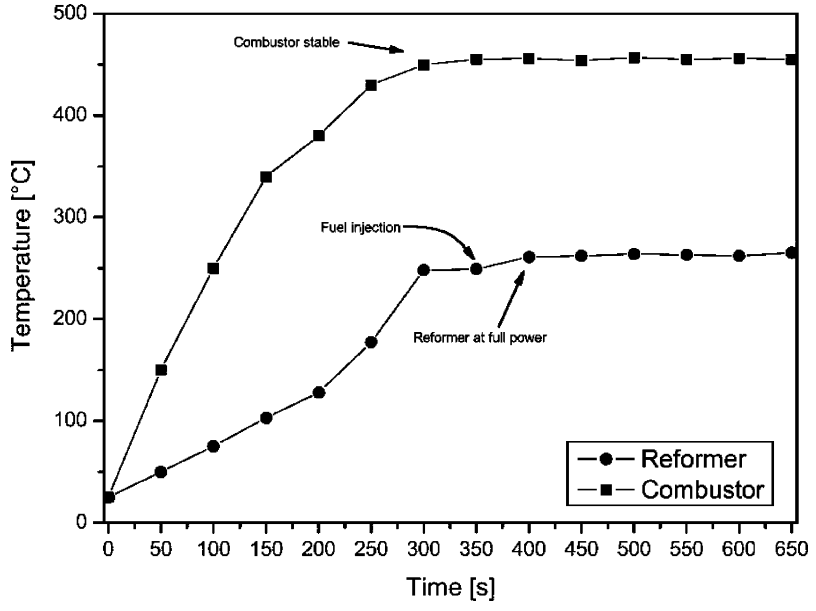

Fig. 7. Temperature profiles in combustor and reformer.

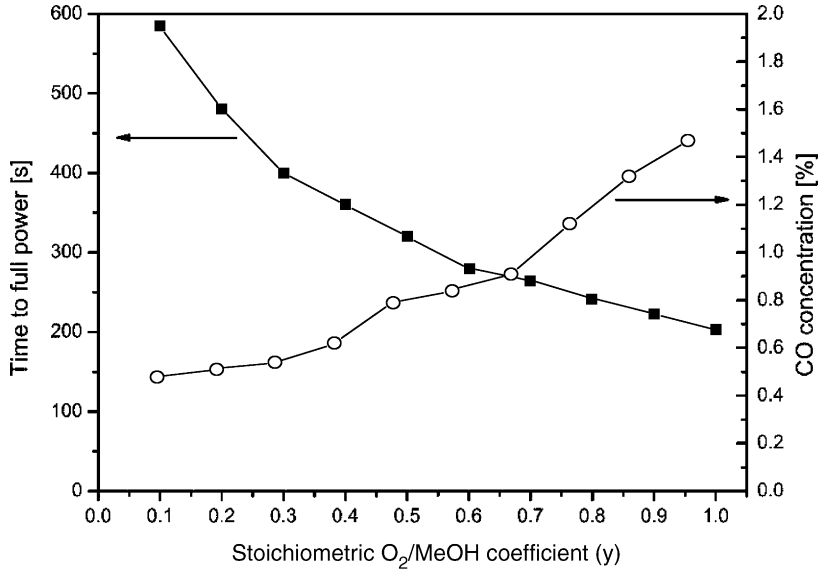

Fig. 8. Influence of oxygen-to-methanol ratio on start-up time and CO concentration ($CH_3OH + xH_2O + 1/2yO_2 \rightarrow (3x + 2y)H_2 + CO_2$).

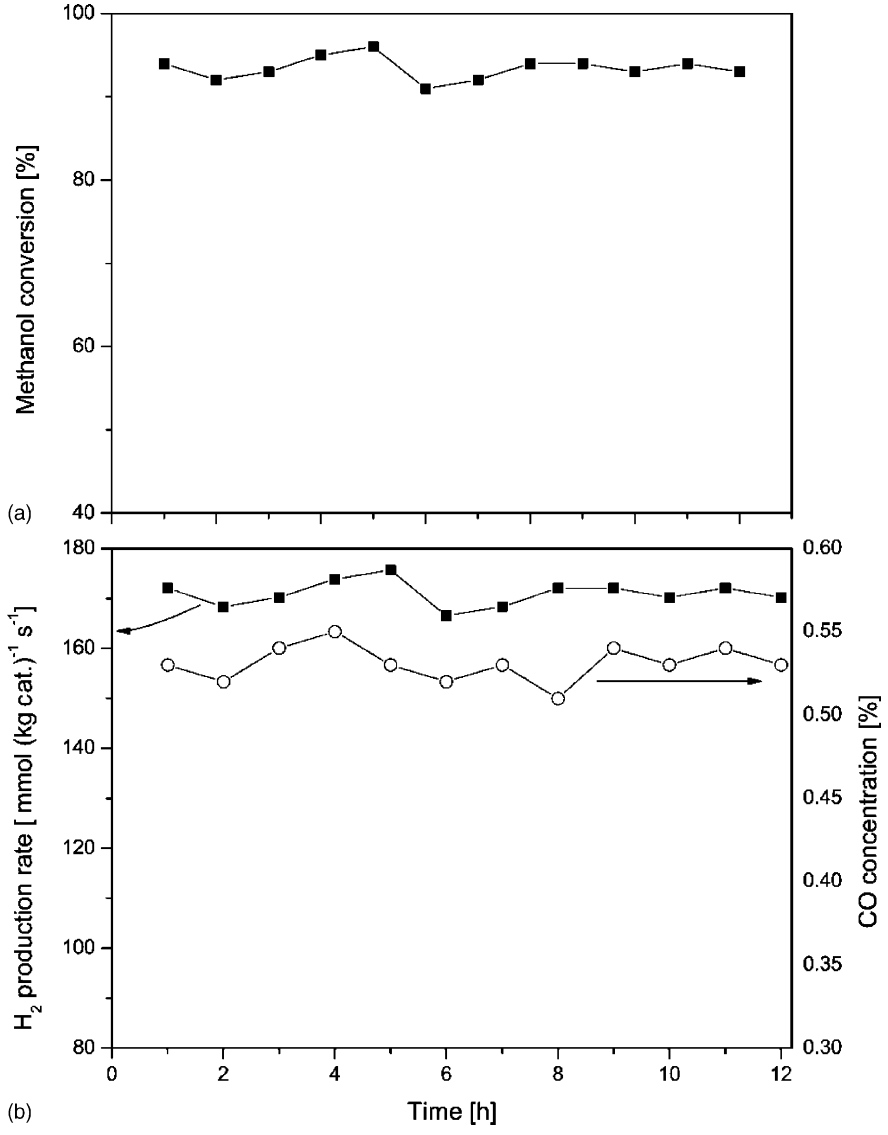

Fig. 9. (a) Stability of methanol conversion, (b) stability of the hydrogen production rate and CO concentration.

4. Conclusions

We have successfully demonstrated that it is possible to obtain reasonable start-up times on a methanol-based reformer without utilizing electrical energy to heat the components of the system. We have shown that it is possible to control the start-up time of the reformer by varying the oxygen-to-methanol ratio, this is however at the expense of increased CO concentrations in the product gas.

The optimal setting for the system was using an oxygen-to-methanol ratio of 0.15 which resulted in a reactor temperature of 260 °C. The conversion was shown to be strongly dependent on the reaction temperature and conversions above 90% were only obtained for temperatures above 250 °C. When increasing the temperature above 260 °C the CO concentrations exceeded the 5000 ppm which was set as an acceptable level at the beginning of this study.

The system showed stability over time as well as over repeated start-up experiments both before and after 12 h studies. The start-up time was also not notably affected by the exposure of the catalyst to the reactants for 12 h.

Acknowledgements

The authors gratefully acknowledge financial support from Volvo Technology Corporation and the Swedish Energy Agency.

References

[1] S. Velu, K. Suzuki, M.P. Kapoor, F. Ohashim, T. Osaki, Appl. Catal. A 213 (2001) 47.
[2] J.C. Amphlett, K.A.M. Creber, J.M. Davis, R.F. Mann, B.A. Peppley, D.M. Stokes, Int. J. Hydrogen Energy 19 (1994) 131.
[3] S.P. Asprey, B.W. Wojciechowski, B.A. Peppley, Appl. Catal. A 179 (1999) 51.
[4] J.P. Breen, F.C. Meunier, J.R.H. Ross, Chem. Commun. 22 (1999) 2247.
[5] C.J. Jiang, D.L. Trimm, M.S. Wainwright, N.W. Cant, Appl. Catal. A 97 (1993) 145.
[6] K. Takahashi, N. Takezawa, H. Kobayashi, Appl. Catal. A 2 (1982) 363.
[7] N. Iwasa, S. Kudo, H. Takahashi, S. Masuda, N. Takezawa, Catal. Lett. 19 (1993) 211.
[8] K. Miyao, H. Onodera, N. Takezawa, React. Kinet. Catal. Lett. 53 (1994) 379.
[9] N. Iwasa, S. Masuda, N. Ogawa, N. Takezawa, Appl. Catal. A 125 (1995) 145.
[10] J. Agrell, K. Hasselbo, S. Järås, M. Boutonnet, Stud. Surf. Sci. Catal. 130 (2000) 1073.
[11] L. Alejo, R. Lago, M.A. Peña, J.L.G. Fierro, Appl. Catal. A 162 (1997) 281.
[12] M.L. Cubeiro, J.L.G. Fierro, Appl. Catal. A 168 (1998) 307.
[13] M.L. Cubeiro, J.L.G. Fierro, J. Catal. 179 (1998) 150.
[14] T.-J. Huang, S.-W. Wang, Appl. Catal. A 40 (1988) 43.
[15] E. Newson, P. Mizsey, T. Truong, P. Hottinger, Stud. Surf. Sci. Catal. 130 (2000) 695.
[16] S. Velu, K. Suzuki, T. Osaki, Catal. Lett. 62 (1998) 159.
[17] S.J. Lee, E.A. Mukerjee, J. McBreen, Electrochim. Acta 44 (1999) 3283.
[18] S. Velu, K. Suzuki, M. Okazaki, M.P. Kapoor, T. Osaki, F. Ohashi, J. Catal. 194 (2000) 373.
[19] S. Murcia-Mascaros, R.M. Navarro, L. Gomez-Sainero, U. Costantino, M. Nocchetti, J.L.G. Fierro, J. Catal. 198 (2001) 338.
[20] T.L. Reitz, S. Ahmed, M. Krumpelt, R. Kumar, H.H. Kung, J. Mol. Catal. 162 (2000) 275.
[21] T.L. Reitz, P.L. Lee, K.F. Czaplewski, J.C. Lang, K.E. Popp, H.H. Kung, J. Catal. 199 (2001) 193.
[22] B. Lindström, L.J. Pettersson, Chem. Eng. Technol., in press.
[23] R.W. McCabe, D.F. McCready, J. Phys. Chem. 90 (1986) 1428.
[24] H.Y.H. Chan, C.T. Williams, M.J. Weaver, C.G. Takoudis, J. Catal. 174 (1998) 191.
[25] H.-B. Zhang, W. Wang, Z.-T. Xiong, G.-D. Lin, Stud. Surf. Sci. Catal. 130 (2000) 1547.
[26] E.D. Guerreiro, O.F. Gorriz, G. Larsen, L.A. Arrúa, Appl. Catal. A 204 (2000) 33.
[27] B. Lindström, L.J. Pettersson, P.G. Menon, Appl. Catal. A 234 (2002) 111.
[28] B. Lindström, L.J. Pettersson, Int. J. Hydrogen Energy 26 (2001) 923.
[29] L. Lloyd, D.E. Ridler, M.V. Twigg, in: M.V. Twigg (Ed.), Catalyst Handbook, Wolfe Publishing, London, 1989, pp. 283–339.